Europe PMC Funders Group Author Manuscript

Sci Transl Med. Author manuscript; available in PMC 2022 January 07.

Published in final edited form as:

Sci Transl Med.; 13(601): . doi:10.1126/scitranslmed.abc3911.

Downregulation of A20 promotes immune escape of lung Adenocarcinomas

Kristina Breitenecker^{#1,2,3}, Monika Homolya^{#1}, Andreea C. Luca^{#1}, Veronika Lang¹, Christoph Trenk¹, Georg Petroczi¹, Julian Mohrherr¹, Jaqueline Horvath¹, Stefan Moritsch^{2,3}, Lisa Haas⁴, Margarita Kurnaeva¹, Robert Eferl^{2,3}, Dagmar Stoiber^{1,5}, Richard Moriggl⁶, Martin Bilban^{7,8}, Anna C. Obenauf⁴, Christiane Ferran^{9,10}, Balazs Dome^{11,12,13}, Viktoria Laszlo^{11,12}, Balázs Gy rffy^{14,15,16}, Katalin Dezso¹⁷, Judit Moldvay^{18,19}, Emilio Casanova^{1,3}, Herwig P. Moll^{1,3,*}

¹Institute of Pharmacology, Center of Physiology and Pharmacology, Medical University of Vienna, AT-1090 Vienna, Austria

²Institute of Cancer Research, Medical University of Vienna, AT-1090 Vienna, Austria

³Comprehensive Cancer Center (CCC), Medical University of Vienna, AT-1090 Vienna, Austria

⁴Research Institute of Molecular Pathology, Vienna Biocenter, AT-1030 Vienna, Austria

⁵Division Pharmacology, Department of Pharmacology, Physiology and Microbiology, Karl Landsteiner University of Health Sciences, AT-3500 Krems, Austria

⁶Institute of Animal Breeding and Genetics, University of Veterinary Medicine, AT-1210 Vienna, Austria

⁷Department of Laboratory Medicine, Medical University of Vienna, AT-1090 Vienna, Austria

⁸Core Facilities, Medical University of Vienna, AT-1090 Vienna, Austria

⁹The Division of Vascular and Endovascular Surgery and the Center for Vascular Biology Research, Department of Surgery, Beth Israel Deaconess Medical Center, Harvard Medical School, Boston MA02215, USA

¹⁰The Transplant Institute and the Division of Nephrology, Beth Israel Deaconess Medical Center, Harvard Medical School, Boston MA 02215, USA

¹¹Division of Thoracic Surgery, Department of Surgery & Comprehensive Cancer Center (CCC), Medical University of Vienna, AT-1090 Vienna, Austria

Author Contributions

KB., MH, ACL and V. Lang designed and performed experiments, CT and GP performed orthotopic transplantations, J. Mohrherr, SM., V. Laszlo and MK performed immunohistochemistry, JH maintained the mouse colonies, KD performed pathological analysis, J. Moldvay prepared the TMA and performed pathological analysis, MB performed RNAseq analysis and helped with data interpretation, LH and ACO performed analysis of the melanoma patient cohort, RE, DS, RM, BG, ACO, CF, and BD provided critical support and corrected the manuscript, EC designed the study, interpreted the data and wrote the manuscript, HPM designed the study, designed and performed experiments, performed GSEA analysis and data mining, interpreted the data and wrote the manuscript.

Competing Interests

The authors declare no competing interests

^{*}To whom correspondence should be addressed at: Herwig P. Moll (HPM), herwig.moll@meduniwien.ac.at. Tel: +43140160-71230, Department of Physiology, Center of Physiology and Pharmacology, Comprehensive Cancer Center, Medical University of Vienna, AT-1090 Vienna, Austria.

¹²1st Department of Tumor Biology, National Korányi Institute of Pulmonology, Semmelweis University, HU-1121 Budapest, Hungary

¹³Department of Thoracic Surgery, National Institute of Oncology and Semmelweis University, HU-1122 Budapest, Hungary

¹⁴MTA TTK Lendület Cancer Biomarker Research Group, Institute of Enzymology & 2nd Department of Pediatrics, Semmelweis University, HU-1117 Budapest, Hungary

¹⁵Department of Bioinformatics, Semmelweis University, HU-1094 Budapest, Hungary

¹⁶2nd Department of Pediatrics, Semmelweis University, HU-1094 Budapest, Hungary

¹⁷1st Department of Pathology and Experimental Cancer Research, Semmelweis University, HU-1085 Budapest, Hungary

¹⁸1st Department of Pulmonology, National Korányi Institute of Pulmonology, HU-1121 Budapest, Hungary

¹⁹SE-NAP Brain Metastasis Research Group, 2nd Department of Pathology, Semmelweis University, HU-1122 Budapest, Hungary

Abstract

Inflammation is a well-known driver of lung tumorigenesis. Tumor cells escape tight homeostatic control by decreasing the expression of the potent anti-inflammatory protein TNFAIP3, also known as A20. Tumor cell intrinsic loss of A20 dramatically enhances lung tumorigenesis and prevents CD8+ T cell mediated immune surveillance in patients and mice. This is completely dependent on increased cellular sensibility to interferon signaling via hyperactivation of TANK-binding kinase 1 (TBK1) and increased expression and activation of STAT1, resulting in elevated PD-L1 expression. Accordingly, immune checkpoint blockade (ICB) is highly efficient in mice harboring A20 deficient lung tumors. Altogether, we have identified A20 as a master immune checkpoint regulating the TBK1-STAT1-PD-L1 axis that may be exploited to improve ICB therapy in lung adenocarcinoma.

Keywords

A20/TNFAIP3; lung adenocarcinoma; K-RAS; inflammation; tumor immune evasion

Introduction

Cancer cells express immune regulatory factors that remodel the tumor microenvironment (TME) and promote tumor immune escape, a hallmark of cancer progression. Accordingly, TME targeting therapies to break tumor-induced immune tolerance are heavily pursued. The development of immune checkpoint inhibitors blocking negative effectors of T cell function was a major advance, especially in malignancies with poor prognosis. In lung cancer, which is the leading cause of cancer related deaths, the approval of immune checkpoint blockade (ICB) raised high hopes and fundamentally changed therapies (1, 2).

[#] These authors contributed equally to this work.

Nevertheless, only around 20% of unselected patients suffering from non-small cell lung cancer (NSCLC) respond to monotherapies targeting Programmed Cell Death Protein 1 (PD-1)/Programmed Death Ligand 1 (PD-L1), and predicting the response of individual patients remains challenging (3–5). A better understanding of factors altering the TME is needed in order to avoid exposing non-responders to the unnecessary toxicity of costly ICB therapeutic regimen.

A number of factors may influence the response to ICB, including mutational burden, the presence of tumor neoantigens, PD-L1 expression in tumor and/or stromal cells and the proportion of tumor-infiltrating immune cells (6–8). Notably, genetic mutations initiating and driving tumor evolution can differently modulate the constitution of the TME (9). This influences the success of ICB treatment and NSCLC patients harboring EGFR mutations or ALK rearrangements notoriously fail immunotherapy (4, 10). Pro-inflammatory, oncogenic K-RAS eventually cooperates with other oncogenes or tumor suppressors to evade tumor immune surveillance. For instance, co-activation of Myc results in the exclusion of cytotoxic T and NK cells with increased infiltration of macrophages (11), while some p53 mutations serve as tumor neoantigens triggering intratumoral T cell responses (12). Loss of STK11/LKB1, a commonly inactivated tumor suppressor in K-RAS driven lung adenocarcinomas (LUAD), results in reduced expression of interferon regulated genes such as T cell chemotactants and PD-L1, which correlate with resistance to ICB (13, 14).

A20, also known as tumor necrosis factor alpha induced protein 3 (TNFAIP3), is a potent anti-inflammatory enzyme and a crucial gatekeeper of inflammation homeostasis (15). Biochemically, A20 exhibits ubiquitin-editing activities, with its N-terminal ovarian tumor (OTU) domain promoting protein de-ubiquitination and the zinc finger motifs at the C-terminus harboring an E3 ligase activity. These properties allow A20 to remove stabilizing K63 linked poly-ubiquitin chains of key NF- κ B signaling components and in turn promote K48 linked ubiquitination, which targets these proteins for proteasomal degradation (15). In addition, A20 interacts with NF- κ B essential modulator (NEMO) and Receptor Interacting Serine/Threonine Kinase 1 (RIP1) through mutual binding to poly-ubiquitin chains in a non-enzymatic manner, thereby inhibiting the phosphorylation of IKK β , which is essential for canonical NF- κ B activation (16, 17). Remarkably, A20 also targets interferon signaling (18, 19), TGF β -induced activation of SMADs (20), and inhibits apoptosis and autophagy, at least in certain cell types (21).

Highlighting the physiological role of A20, various polymorphisms of the A20/TNFAIP3 gene resulting in reduced expression of functional gene product are linked to inflammatory and autoimmune diseases (22, 23). With respect to cancers, A20's role remains controversial, i.e. oncogenic or tumor suppressive depending on the tissue of origin (24–29). In this work, we discovered a novel function for A20 in NSCLC. Our data show that tumor intrinsic downregulation or loss of A20 promotes the growth of LUAD by facilitating tumor immune evasion in a TBK1-STAT1-PD-L1 dependent manner. Thus, A20 is a potent immune checkpoint and its tumor intrinsic expression levels may influence the outcome of anti-PD-L1 based therapies in LUAD.

Results

A20 is a tumor suppressor in K-RAS driven lung tumorigenesis

Analysis of LUAD patient data derived from the Cancer Genome Atlas (TCGA) revealed two patients harboring K-RAS driver mutation and concomitant deep deletion of the TNFAIP3 gene, encoding for A20. 55.40% of K-RAS driven LUAD exhibited shallow/ heterozygous deletion of the TNFAIP3 gene, suggesting that tumors aim to escape the A20 mediated negative feedback loop of NF- κ B activation (Fig. 1A&B). Indeed, when we compared gene expression of LUAD with patient-matched adjacent, non-malignant lung tissues (GSE75037), we noticed downregulation of A20 mRNA in tumor tissues, irrespective of K-RAS or EGFR mutations (Fig. 1C). Meta-analysis of different LUAD studies further confirmed downregulation of A20 in tumor tissue (Fig. S1A). A20 expression in K-RAS mutant, EGFR mutant and K-RAS/EGFR wildtype (wt) tumors was similar (Fig S1B). Remarkably, very low A20 expression in unselected LUAD tumors patients resulted in worse prognosis (Fig. 1D) (30).

To test potential tumor-intrinsic suppressive properties of A20 expression experimentally, we crossed K-ras^{G12D} mice (K) (31) with A20 floxed/floxed mice (hereafter KA mice) (32, 33). Recombination in lung epithelial cells was achieved following intranasal inhalation with Cre expressing adenovirus, which resulted in concomitant K-ras^{G12D} activation and A20 deletion in expanding tumor cell populations in K-ras^{G12D}:A20 Lep: Lep mice (Lep: deletion in lung epithelial cells). Mice harboring A20 deficient tumors, as well as A20 heterozygous tumors, exhibited dramatically reduced survival as compared to mice with A20 proficient tumors (Fig. 1E). Since A20 may affect p53 expression (34), we crossed K and KA mice with p53 floxed/floxed mice, yielding KP and KPA mice respectively. P53 restrains tumor progression, hence KP mice develop advanced adenocarcinomas more closely recapitulating advanced human LUAD as compared to tumors in K mice (35). Our data indicate that A20 knockout still enhanced tumorigenesis to further reduce mice survival in KPA vs. KP mice (Fig. 1F). Of note, we did not see gender-related effects on survival (Fig S1C). Histologically, KA and KPA mice suffer from increased tumor burden compared to controls when analyzed 10 weeks post tumor induction (Fig. 1G & S1D). Indeed, tumor intrinsic loss of A20 resulted in increased lung to body weight ratio, tumor to lung area ratio, tumor numbers per analyzed section and increased average tumor size (Fig. 1H & Fig. S1E). Furthermore, advanced grade II/III tumors were more abundant in KA mice as compared to K mice (Fig. 1I). As in humans, mouse lung tumors displayed a downregulation of A20 expression in comparison to healthy wt lungs (Fig. 1J&K, Fig. S1F). Taken together, these data identify a potent tumor suppressive role of A20 in the development of K-RAS driven LUAD.

Loss of A20 alters tumor immune cell infiltration

Next, we performed IHC analysis for the proliferation marker Ki67 in lungs 10 weeks post tumor initiation. Intriguingly, in both K and KP mice deletion of A20 resulted in rather decreased proliferation, even reaching significance in KP mice (Fig. 2A&B). However, stainings for Cleaved Caspase 3 (CC3) revealed substantial reduction of apoptotic cells in A20 knockout tumors. *In vitro*, isolated cells from KP, KPA and KPA (HET) tumors

proliferated at the same pace (Fig. S2A). Reduced A20 expression in KPA (HET) cells, which are heterozygous for A20, and complete recombination of the floxed A20 allele was confirmed by Western blot and PCR (Fig. S2B). Also the K-RAS mutated mouse LUAD cell line (368T1) and human A549 cells did not show alterations in proliferation or apoptosis assays in vitro upon CRISPR-Cas9 mediated A20 knockout (Fig. S2C-D). Moreover, we did not observe a difference in tumor growth of these cells when subcutaneously transplanted into NOD scid gamma (NSG) mice (Fig. 2C&S2F), although control cells still expressed detectable levels of A20 in the immunodeficient recipients (Fig. S2G). Hence, we reasoned that tumor infiltrating immune cells contribute to the tumor suppressive properties of A20. Analysis of immune cell composition in autochthonous tumor bearing KP and KPA-derived lungs by flow cytometry revealed no difference in CD45⁺ cell numbers upon tumor specific A20 knock-out. However, the composition of these immune cells was totally shifted towards a pro-tumorigenic phenotype in A20 knock-out compared to A20 expressing LUAD. Indeed, we noticed an increase of neutrophilic myeloid derived suppressor cells (MDSC, CD11b+Ly6G+LyGC-) in KPA tumor bearing lungs concomitant with decreased levels of cytotoxic CD8⁺ T cells and NK cells (Fig. 2D & Fig. S2H).

A20 expression positively correlates with cytotoxic T cell infiltration in LUAD patients

Having shown that loss of A20 in K-ras driven mouse LUAD tumors results in an immunosuppressive TME, we questioned whether these results translate to human patients. Therefore, we subjected gene expression data of 83 LUAD samples (GSE75037 cohort) to CIBERSORT analysis (36, 37), and correlated results with respective A20 expression. Interestingly, high A20 expression associated with a bona fide tumor suppressive immune phenotype, characterized by higher abundance of CD8+ T cells, M1 macrophages and NK cells, but lower levels of M2 macrophages and regulatory T cells (Fig. 3A & Fig. S3A). Notably, this A20 – immune cell correlation was restricted to tumor tissues. In the adjacent healthy lung parenchyma, A20 only positively correlated with M1 macrophages, and, in contrast to the tumor tissue, inversely correlated with NK cells (Fig. S3B). Given the increased CD8⁺ T cell abundance in LUAD biopsies with elevated A20 expression, we checked the immune cytolytic activity as defined by the mean expression of perforin-1 (PRF-1) and granzyme A (GZMA) mRNA (38). Again, we noticed a strong positive correlation with A20 expression in LUAD biopsies but not in the healthy lung parenchyma (Fig. 3B). However, the analysis of bulk gene expression data does not allow distinction between tumor cell- or stromal-derived A20 expression. Therefore, we analyzed 76 human unselected LUAD biopsies spotted on tissue microarrays by IHC for A20 and CD8 expression/infiltration. Unbiased grading by two double blinded pathologists (JM&KD) revealed lower CD8⁺ T cell abundance when tumors exhibited low A20 expression compared to tumors with higher A20 expression (Fig. 3C&D). Notably, A20 expression in immune cells did not affect the abundance of CD8⁺ T cells in these LUAD biopsies (Fig. S3C). A20 protein in the tumor cells also positively correlated with the expression of PD-L1 (39), a potential surrogate marker for the infiltration of cytotoxic T cells (Fig. 3E). Indeed, mRNA expression analysis of K-RAS mutant LUAD biopsies showed a strong positive correlation between CD8A and PD-L1 as well as with its main regulator IFN γ (Fig S3D), and the expression of all three genes correlated positively with A20 (Fig. S3E).

Nevertheless, based on these patient derived data, we cannot yet conclude that low A20 expression results in low T cell based immune surveillance. A20 may also be expressed in tumor cells in response to infiltrating T cells, being low A20 levels a consequence of weak infiltration of cytotoxic cells, rather than the cause. To address this question, we analyzed the genetic status of A20 and its correlation with CD8⁺ tumor infiltrating cells in the TCGA LUAD data-set using gene set enrichment analysis (GSEA). We discriminated between K-RAS mutant patients with somatic shallow TNFAIP3/A20 deletions ("HET", n=79) characterized by impaired A20 expression in the tumors, and K-RAS mutant patients without genetic aberrations in the TNFAIP3 gene ("WT", n=61). Strikingly, a gene signature including the 100 most significantly genes correlating with high CD8⁺ abundance in LUAD samples (37) was enriched in "WT" patients, and *vice versa*, genes correlating with low CD8⁺ T cell abundance were enriched in "HET" patients (Fig. 3F, and suppl. table 1&2). Taken together, these data indicate that impaired A20 expression facilitates the tumor to escape T cell mediated immune surveillance.

Increased tumorigenicity of A20 knockout LUAD depends on evasion of CD8+ T cells

Given the correlation between tumor cell intrinsic A20 expression and T cell infiltration in human LUAD, we questioned whether decreased tumor immune surveillance contributes to enhanced tumor growth in our mouse models. First, we confirmed decreased CD3+ T cell infiltration upon knock out of A20 in the lung tumors of mice 10 weeks post activation of oncogenic K-ras (Fig. 4A). Although loss of p53 eventually modulates myeloid cells within the tumor immune microenvironment (TIME), as well as regulatory T cells (40), it was shown for the K-ras^{G12D} LUAD mouse model that p53 deficiency does not significantly influence the composition of the TIME (9). Thus, KPA displayed decreased T cell infiltration compared to KP tumors, similar as in KA versus K mice (Fig. 4B). In accordance, we noticed decreased CD8+ abundance in KPA versus KP tumors, concomitant with a decrease of the cytotoxic immune mediators Gzma, Gzmb and Prf-1 (Fig. 4C&D). Next, we performed orthotopic transplants of KP and KPA cells into immunodeficient NSG mice, as well as into immunocompetent, syngeneic C57Bl/6 mice. As in the subcutaneous grafts, we did not observe an effect of A20 knockout in NSG mice, but noticed a striking difference in the survival of immunocompetent mice (Fig. 4E). Consistently, in the latter model increased growth of KPA tumors was accompanied by the exclusion of CD8+ T cells, starting two weeks after transplantation (Fig. S4). Therefore, we depleted CD8⁺ T cells in C57Bl/6 recipients of KP and KPA cells 1 week following transplantation. While this treatment did not affect the survival of mice engrafted with KPA cells, it decreased the life of KP recipients to a similar extend as tumor cell intrinsic A20 knockout (Fig. 4F). In line, in autochthonous LUAD induced by Ad.Spc-Cre, KP mice exhibited a tumor load (lung/body weight ratio and tumor number) comparable to KPA mice upon CD8⁺ T cell depletion (10 weeks treated) but increased in comparison to isotype treated KP mice, whereas this had no obvious effects in KPA mice (Fig 4G&H).

Autocrine IFN signaling enables aberrant growth of A20 knockout LUAD

Next, we aimed to understand the molecular mechanisms mediating intratumoral A20 downregulation and tumor immune evasion. We used an inflammatory antibody array and analyzed protein lysates of macroscopically dissected KP and KPA tumors. However, we

could not detect differences in the expression of any of the 40 cytokines spotted on the array (Fig. S5A). Therefore, we performed RNAseq and subsequent gene set enrichment analysis (GSEA) for hallmark gene sets and found only two sets enriched in KPA versus KP lungs, namely the gene sets for IFN γ and IFN α response (Fig. 5A and Fig. S5B&C). Importantly, while the expression of different type I Ifn was below detection limit in the tumors, Ifny mRNA remained unchanged in KP versus KPA tumors at this time point (Fig. S5D), suggesting that A20 deficient LUAD cells are more sensitive to Ifnγ. We and others previously reported A20-mediated regulation of STAT1 expression and downstream response to IFN signaling in different cellular contexts (19, 33). In line with these, KPA LUAD cells also exhibited elevated Stat1 expression at baseline and activated Stat1 upon Ifnγ stimulation resulting in increased expression of the IFNγ target genes Pd-l1 and Ido following 4 hours of Ifny stimulation (Fig 5B&S5E). The expression of these STAT1 regulated genes was independent of p65 expression, since p65 deficient KPA cells also exhibited higher Stat1, Pd-11 and Ido expression as compared to p65 knock-out KP cells (Fig. 5B & S5F). Increased activation of Stat1 in KPA versus KP and KPA p65 versus KP p65 was confirmed on protein level (Fig. 5C). Notably, Pd-l1 is a member of the IFNy response hallmark gene set, and its expression was induced in autochthonous KPA tumors 10 weeks after tumor induction, when Ifny levels were comparable between KP and KPA tumors, and in orthotopically transplanted KPA cells two weeks post engraftment (Fig. S5C, D, G-I). However, at a later time point when orthotopically transplanted KPA tumors were already devoid of CD8+ T cells, Pd-11 expression in KPA tumor cells decreased as compared to KP cells (Fig S4 & S5I).

We previously reported for vascular cells that A20 controlled TBK1 activity, which is upstream of an autocrine IFN β /IFNAR loop transcriptionally regulating STAT1 expression (Fig. 5D) (19, 41). Indeed, Tbk1 phosphorylation at S172 was elevated in KPA cells, independent of p65 expression, compared to KP cells (Fig. 5E). Moreover, blocking Tbk1 activation using the TBK1/IKK- ϵ specific inhibitor amlexanox in KPA cells prevented increased Stat1 expression and phosphorylation, as well as the elevated downstream expression of Pd-11 (Fig 5F & Fig S5J) (42). Thus, it appeared that knockout of A20 primed LUAD cells to IFN γ in a TBK1-dependent but NF- κ B-independent manner.

To investigate whether this mechanism contributes to the evasion of KPA tumors from CD8 $^+$ T cell infiltration, we generated KP and KPA cells deficient for the IFN type I receptor Ifnar, thereby abrogating autocrine Ifn β signaling (Fig S5K). Hence, these cells fail priming for strong Ifn γ mediated responses (43), indicated by reduced Stat1 expression in KPA ^{Ifnar} versus KPA cells (Fig. 5G). When transplanting KP ^{Ifnar} and KP cells into immunocompetent mice, we noticed that blocking baseline type I Ifn signaling in the tumor cells did not modify the composition of the TIME, as analyzed two weeks following engraftment by flow cytometry. However, Ifnar deletion in KPA cells restored CD8 $^+$ T cell infiltration, suggesting that increased activation of type I Ifn is responsible for the exclusion of cytotoxic T cells in KPA tumors (Fig. 5H & S5L). Furthermore, we crossed Ifnar floxed/floxed mice (44) with K mice to generate Ifnar-deficient, K-ras-driven tumors following Ad.Spc-Cre inhalation. Kaplan Meier analysis and lung sections prepared 10 weeks post tumor initiation revealed no impact of Ifnar deletion in K-ras lung tumorigenesis and progression (Fig. 5I&S5M). However, when we crossed KA mice with Ifnar floxed

mice, we observed better survival along with decreased lung/body weight ratios and tumor burden, and increased infiltration of CD3⁺ cells upon Ifnar ablation in KA tumor cells (Fig. 5J-M). These results further demonstrate that alterations in IFN signaling are critical for the tumor suppressor function of A20, regardless of the p53 status.

A20 deficiency sensitizes LUAD to anti-PD-L1 therapy

Enhanced IFN signaling in the tumor tissue was associated with a better response of NSCLC patients to PD-1/PD-L1 targeting ICB (45, 46). Data from melanoma patients also suggested an essential role of tumor cell intrinsic IFN signaling in the response to immunotherapy (47–50). Based on the RNAseq results we created an A20 Loss of Function (LOF) signature including the genes significantly up- and downregulated in KPA versus KP lungs 10 weeks post tumor initiation. Intriguingly, melanoma patients with higher A20 LOF signature responded better to PD-1 blockade, as illustrated by overall survival, as well as progression free survival (Fig. 6A) (51). To check whether KPA LUAD respond to ICB, we generated KP and KPA cell lines deficient of Pd-11 (Fig. S6A). Subsequent orthotopic transplantation of KPA Pd-11 in syngeneic C57B1/6 mice resulted in increased survival compared to recipients of KPA cells and similar survival compared to recipients of KP cells (Fig. 6B). Notably, Pd-11 deletion in KP cells did not extend the life of recipients in this model. However, in agreement with our previous analysis of the TIME upon Ifnar or Stat1 deletion (Fig. 5H, S5L & S6B), Pd-11 deletion restored the infiltration of CD8+ T cells in KPA tumors (Fig. 6C). Surprisingly, we did not find any alteration in the TIME of KP cells upon Pd-11 or Stat1 deletion, and the application of α-Pd-11 antibodies yielded similar results (Fig. 6D & S6C, D). Furthermore, we treated KP and KPA mice bearing autochthonous tumors for a 10 week period with the α -Pd-l1 antibody. As in the transplant model, we observed no beneficial effect in KP mice, but α-Pd-l1 treatment reduced lung to body weight ratios, tumor number and burden in KPA mice, as compared to mice treated with isotype antibody (Fig. 6E&F). Additionally, \alpha-Pd-11 treatment restored T cell infiltration in KPA mice as confirmed by IHC using CD3 marker (Fig. 6G&H).

Altogether, our data suggest that A20 is a prominent regulator of the TBK1/STAT1 axis and thereby prevents tumor immune evasion. However, low A20 expression in tumors results in an increased IFN γ expression gene signature that renders these tumors more vulnerable to ICB therapy.

Discussion

Our results uncovered a tumor suppressor function of A20 in LUAD. In humans, tumors show reduced levels of A20 compared to healthy parenchyma regions, indicating that downregulation of A20 promotes tumor progression. Importantly, reduced A20 expression levels correlated with worse patient prognosis. In agreement, deletion of A20 in mouse models of *K-ras* driven LUAD enhanced tumorigenesis, independently of p53 expression. Since inflammation is generally considered as a major oncogenic factor (52), it is tempting to speculate that loss of anti-inflammatory A20 may drive carcinogenesis in other (lung-) tumors as well. However, this needs to be verified experimentally and our analysis can only conclude for LUAD.

In previous studies, genetic deletion of the p65 subunit, expression of inhibitor kappa B (I κ B) super repressor gene and chemical inhibition of I κ B kinase (IKK) activity inhibited lung tumorigenesis in the K and in the more aggressive KP mice, underscoring the importance of tumor intrinsic NF- κ B signaling in these models (53–56). However, despite being a potent suppressor of NF- κ B activation (15), A20 knockout did not induce changes in proliferation and apoptosis of cell lines. On the other hand, *in vivo* deletion of A20 in LUAD shaped the TIME towards a more immunosuppressive phenotype, resulting in lower CD8+ T tumor infiltrating cell proportions and reduced tumor cell apoptosis levels, providing an explanation for the observed tumor suppressor function of A20. These results were confirmed in human LUAD biopsies, where low A20 expression levels and loss of A20 heterozygosity correlated with reduced CD8+ T cell numbers and immune-cytolytic activity.

More than 50% of K-RAS mutant tumors included in the TCGA cohort exhibited shallow deletions of A20, which are defined as "possibly a heterozygous deletion". In contrast, homozygous deletions were rare. This may be explained by the importance of surrounding genes of A20 at its localization on chromosome 6. (57) Notably, IFNGR1 is located in close proximity, hence deep deletion of this chromosomal locus may also abrogate IFN signaling, thereby counteracting the impact of A20 downregulation. Indeed, in our models we found type I and type II IFN target genes being enriched in A20 knockout tumors compared to A20 proficient LUAD, despite equal IFN levels in both groups. Tonic type I IFN signaling primes cells for strong IFNy responses via regulation of STAT1 expression (41, 58), and STAT1 is increasingly expressed and activated upon A20 knockout, independent of canonical NF-κB, but dependent on TBK1 activation, as previously observed in vascular cells (19). Increased cellular sensitization to IFN γ will impact the immune cell composition within the TME and can contribute to tumor immune evasion. Indeed, we observed alteration of MDSC, NK and T cells upon A20 deficiency in our autochthonous LUAD mouse models. These changes were restricted to the decreased infiltration of CD8⁺ T cells observed upon orthotopic transplantation of KPA cells, which may be related to the fast progression of tumors in this model. Consistently with these results, disruption of the TBK1/IFN/STAT1 axis via deletion of IFNAR or STAT1 restored tumor immune surveillance in A20-deficient LUAD.

Although the activation of TBK1 in A20 knockout cells is intriguing, more experiments are needed to clarify the exact mechanisms in LUAD cells. One possibility would be the lack of A20 mediated disruption of the TRAF3-TBK1 complex, a prerequisite for TBK1 phosphorylation, as described in mouse embryonic fibroblasts (18). It is also possible that loss of A20 stabilizes TBK1 upstream activators such as STING or other components of the Toll-like receptors signaling pathway (59).

IFNs have a complex role in tumorigenesis. It is well accepted that IFN γ , primarily produced by activated T cells, NK and NKT cells can be anti-tumorigenic thanks to its anti-proliferative and pro-apoptotic properties. In addition, IFN γ may facilitate anticancer immunity through its immunomodulatory actions and the upregulation of cytotoxic enzymes (60). However, IFN γ also induces the tumor cell intrinsic expression of PD-L1 in a STAT1-dependent manner, favoring the immune escape of these cells. The balance between pro-and anti-tumorigenic effects of IFN γ /STAT1 signaling are context-dependent and may be governed by threshold levels, by the immune composition of the TME and/or by temporal

events during tumorigenesis (61). The strong expression of IFNy regulated genes PD-L1, IDO and others immune suppressive molecules may contribute to the positive selection of low A20 expressing lung tumor cells and to abrogate the antitumor immune response during tumorigenesis. However, this elevated IFN γ sensitivity also renders the tumors more susceptible to ICB. Indeed, previous reports have identified an IFNy induced gene signature as predictor to responses to ICB (45, 46, 49) and analysis of our experimental models revealed that A20 deletion in tumor cells also enhances PD-L1 expression in a STAT1 dependent manner. Thus, we reasoned that the effect of A20 loss may be counteracted by ICB treatment. Indeed, genetic deletion of PD-L1 in K-ras mutated LUAD cells and pharmacological blocking of PD-L1 rescued the A20 tumor suppressor function by reestablishing T cell infiltration and reducing tumorigenesis in syngeneic orthotopic mouse models and in K-ras mutated A20 knockout animals harboring autochthonous tumors. Notably, targeting Pd-11 in KPA tumors yielded results comparable to A20 expressing KP tumors. Intriguingly, we could not observe any effect of targeting Pd-11 in A20 expressing tumors. This may be explained by the low mutational burden and lack of strong neoantigens, hence the minor role of regulatory T cells in these models (62, 63), or by different experimental conditions.(64)

In our experimental models, loss of A20 sensitize the tumors to anti PD-L1 treatment. In this line, an A20 LOF signature derived from A20 knockout lung tumors predicts response to ICB in melanoma patients. On the other hand, we also noticed a positive correlation between A20 and PD-L1 expression in human tumors. We speculate that most of the low A20 expressing tumors already escaped immune surveillance and are devoid of IFN γ producing CD8⁺ cells, therefore expressing low levels of PD-L1. This would suggest that patients with K-RAS mutated and low A20 expressing cold tumors may not response to anti-PD-L1 treatment as monotherapy, but could require immunogenic chemotherapies in addition to ICB to re-activate infiltration of cytotoxic T cells (65–67) and for maximal therapeutic benefit.

The lack of clinical data derived from LUAD patients undergoing ICB therapy limits this study. Our findings that A20 LOF signature predict ICB response in melanoma patients are encouraging, but may not be translated into LUAD patients. Future studies analyzing the implications of A20, and its downstream targets TBK1 and STAT1, in LUAD patients treated with ICB alone or combined with chemotherapy will help elucidating whether A20 expression in tumor cells can be exploited as marker to identify LUAD patients that benefit from ICB therapy.

Materials And Methods

Study design

The rational of the study was to investigate the impact of anti-inflammatory A20 in lung tumorigenesis. We used publically available patient datasets and patient biopsies for the acquisition of human data. Experimental data was acquired from mouse models and *in vitro* models based on the knock-out of A20 in lung tumor cells. For all animal experiments, required samples sizes were determined by using web-based tools (http://www.cct.cuhk.edu.hk/stat/survival/Rubinstein1981.htm and http://

www.quantitativeskills.com/sisa/calculations/samsize.htm). Calculated sample numbers were adjusted according to the availability of mice and in accordance with the 3 Rs. For antibody mediated depletion studies and anti-Pd-l1 treatment, mice were randomly assigned mice to the different treatment groups. Tissue was harvested and processed in a random and blinded order. Generally, all replicates were included in our data analysis, but data points less than $Q1 - 1.5 \times IQR$ or greater than $Q3 + 1.5 \times IQR$ were considered as outliers and from statistical analysis.

Statistical analysis

We used GraphPad Prism 5.0 for statistical analysis. Unless stated otherwise in the figure legends, all values are given as means \pm SD. Comparisons between two groups were made by Student's t test, except for Kaplan-Meier analysis, where the log rank test was used. To compare more than two groups, we used Oneway ANOVA with subsequent Tukey's multiple comparison. To measure significant correlations between two variables, we determined the Pearson correlation coefficient. P values <0.05 were considered as significant.

Supplementary Material

Refer to Web version on PubMed Central for supplementary material.

Acknowledgments

We thank Safia Zahma who provided help for the preparation of tissue sections, Barbara Dekan for help with the stainings of the TMA, as well as Markus Jeitler and Sophia Derdak for help with RNA-Seq analysis.

Funding

This project was supported by the Initiative Krebsforschung Research Grant and the Fellinger Krebsforschung to HPM and the Austrian Science Fund (FWF, P33430 and 32900 to EC and HPM, P25599-B19, P32900 and Doc59-B33 to EC, SFB-F04707, SFB-F06105 and I4157-B to RM, I3522 to V.Laszlo, I3977 and I4677 to BD). BG was supported by the KH129581 grant of the National Research, Development and Innovation Office, Hungary. V. Laszlo is a recipient of Janos Bolyai Research Scholarship of the Hungarian Academy of Sciences and the UNKP-19-4 New National Excellence Program of the Ministry for Innovation and Technology. J. Moldvay was supported by the Hungarian NRDI Office (Grant OTKA-K129065).

Data And Materials Availability

All materials will be made available to the scientific community. RNA-seq data are deposited in the GEO repository (GSE148194).

References

- 1. Herbst RS, Morgensztern D, Boshoff C. The biology and management of non-small cell lung cancer. Nature. 2018; 553:446–454. [PubMed: 29364287]
- 2. Ott PA, Hodi FS, Kaufman HL, Wigginton JM, Wolchok JD. Combination immunotherapy: a road map. Journal for immunotherapy of cancer. 2017; 5:16. [PubMed: 28239469]
- 3. Prelaj A, Tay R, Ferrara R, Chaput N, Besse B, Califano R. Predictive biomarkers of response for immune checkpoint inhibitors in non-small-cell lung cancer. European journal of cancer (Oxford, England: 1990). 2019; 106:144–159.
- 4. Borghaei H, Paz-Ares L, Horn L, Spigel DR, Steins M, Ready NE, Chow LQ, Vokes EE, Felip E, Holgado E, Barlesi F, et al. Nivolumab versus Docetaxel in Advanced Nonsquamous Non-Small-

- Cell Lung Cancer. The New England journal of medicine. 2015; 373:1627–1639. [PubMed: 26412456]
- Garon EB, Rizvi NA, Hui R, Leighl N, Balmanoukian AS, Eder JP, Patnaik A, Aggarwal C, Gubens M, Horn L, Carcereny E, et al. Pembrolizumab for the treatment of non-small-cell lung cancer. The New England journal of medicine. 2015; 372:2018–2028. [PubMed: 25891174]
- 6. Luksza M, Riaz N, Makarov V, Balachandran VP, Hellmann MD, Solovyov A, Rizvi NA, Merghoub T, Levine AJ, Chan TA, Wolchok JD, et al. A neoantigen fitness model predicts tumour response to checkpoint blockade immunotherapy. Nature. 2017; 551:517–520. [PubMed: 29132144]
- 7. Taube JM, Klein A, Brahmer JR, Xu H, Pan X, Kim JH, Chen L, Pardoll DM, Topalian SL, Anders RA. Association of PD-1, PD-1 ligands, and other features of the tumor immune microenvironment with response to anti-PD-1 therapy. Clinical cancer research: an official journal of the American Association for Cancer Research. 2014; 20:5064–5074. [PubMed: 24714771]
- 8. Hwang S, Kwon AY, Jeong JY, Kim S, Kang H, Park J, Kim JH, Han OJ, Lim SM, An HJ. Immune gene signatures for predicting durable clinical benefit of anti-PD-1 immunotherapy in patients with non-small cell lung cancer. Scientific reports. 2020; 10:643. [PubMed: 31959763]
- Busch SE, Hanke ML, Kargl J, Metz HE, MacPherson D, Houghton AM. Lung Cancer Subtypes Generate Unique Immune Responses. Journal of immunology (Baltimore Md 1950). 2016; 197 :4493–4503.
- 10. Gainor JF, Shaw AT, Sequist LV, Fu X, Azzoli CG, Piotrowska Z, Huynh TG, Zhao L, Fulton L, Schultz KR, Howe E, et al. EGFR Mutations and ALK Rearrangements Are Associated with Low Response Rates to PD-1 Pathway Blockade in Non-Small Cell Lung Cancer: A Retrospective Analysis. Clinical cancer research an official journal of the American Association for Cancer Research. 2016; 22:4585–4593. [PubMed: 27225694]
- 11. Kortlever RM, Sodir NM, Wilson CH, Burkhart DL, Pellegrinet L, Brown Swigart L, Littlewood TD, Evan GI. Myc Cooperates with Ras by Programming Inflammation and Immune Suppression. Cell. 2017; 171:1301–1315. e1314 [PubMed: 29195074]
- 12. Dong ZY, Zhong WZ, Zhang XC, Su J, Xie Z, Liu SY, Tu HY, Chen HJ, Sun YL, Zhou Q, Yang JJ, et al. Potential Predictive Value of TP53 and KRAS Mutation Status for Response to PD-1 Blockade Immunotherapy in Lung Adenocarcinoma. Clinical cancer research: an official journal of the American Association for Cancer Research. 2017; 23:3012–3024. [PubMed: 28039262]
- Skoulidis F, Goldberg ME, Greenawalt DM, Hellmann MD, Awad MM, Gainor JF, Schrock AB, Hartmaier RJ, Trabucco SE, Gay L, Ali SM, et al. STK11/LKB1 Mutations and PD-1 Inhibitor Resistance in KRAS-Mutant Lung Adenocarcinoma. Cancer discovery. 2018; 8:822– 835. [PubMed: 29773717]
- 14. Kitajima S, Ivanova E, Guo S, Yoshida R, Campisi M, Sundararaman SK, Tange S, Mitsuishi Y, Thai TC, Masuda S, Piel BP, et al. Suppression of STING Associated with LKB1 Loss in KRAS-Driven Lung Cancer. Cancer discovery. 2019; 9:34–45. [PubMed: 30297358]
- 15. Ma A, Malynn BA. A20: linking a complex regulator of ubiquitylation to immunity and human disease. Nature reviews Immunology. 2012; 12:774–785.
- Skaug B, Chen J, Du F, He J, Ma A, Chen ZJ. Direct, noncatalytic mechanism of IKK inhibition by A20. Molecular cell. 2011; 44:559–571. [PubMed: 22099304]
- 17. Enesa K, Moll HP, Luong L, Ferran C, Evans PC. A20 suppresses vascular inflammation by recruiting proinflammatory signaling molecules to intracellular aggresomes. Faseb j. 2015; 29:1869–1878. [PubMed: 25667218]
- 18. Parvatiyar K, Barber GN, Harhaj EW. TAX1BP1 and A20 inhibit antiviral signaling by targeting TBK1-IKKi kinases. J Biol Chem. 2010; 285:14999–15009. [PubMed: 20304918]
- Moll HP, Lee A, Minussi DC, da Silva CG, Csizmadia E, Bhasin M, Ferran C. A20 regulates atherogenic interferon (IFN)-gamma signaling in vascular cells by modulating basal IFNbeta levels. J Biol Chem. 2014
- 20. Bhattacharyya S, Wang W, Graham LV, Varga J. A20 suppresses canonical Smad-dependent fibroblast activation: novel function for an endogenous inflammatory modulator. Arthritis research & therapy. 2016; 18:216. [PubMed: 27716397]
- 21. Priem D, van Loo G, Bertrand MJM. A20 and Cell Death-driven Inflammation. Trends Immunol. 2020; 41:421–435. [PubMed: 32241683]

 Musone SL, Taylor KE, Lu TT, Nititham J, Ferreira RC, Ortmann W, Shifrin N, Petri MA, Kamboh MI, Manzi S, Seldin MF, et al. Multiple polymorphisms in the TNFAIP3 region are independently associated with systemic lupus erythematosus. Nature genetics. 2008; 40:1062– 1064. [PubMed: 19165919]

- 23. Zhou Q, Wang H, Schwartz DM, Stoffels M, Park YH, Zhang Y, Yang D, Demirkaya E, Takeuchi M, Tsai WL, Lyons JJ, et al. Loss-of-function mutations in TNFAIP3 leading to A20 haploinsufficiency cause an early-onset autoinflammatory disease. Nature genetics. 2016; 48:67–73. [PubMed: 26642243]
- 24. Lee JH, Jung SM, Yang KM, Bae E, Ahn SG, Park JS, Seo D, Kim M, Ha J, Lee J, Kim JH, et al. Park, A20 promotes metastasis of aggressive basal-like breast cancers through multimonoubiquitylation of Snail1. Nature cell biology. 2017; 19:1260–1273. [PubMed: 28892081]
- 25. Schmitz R, Hansmann ML, Bohle V, Martin-Subero JI, Hartmann S, Mechtersheimer G, Klapper W, Vater I, Giefing M, Gesk S, Stanelle J, et al. TNFAIP3 (A20) is a tumor suppressor gene in Hodgkin lymphoma and primary mediastinal B cell lymphoma. The Journal of experimental medicine. 2009; 206:981–989. [PubMed: 19380639]
- Nakagawa MM, Rathinam CV. A20 deficiency in hematopoietic stem cells causes lymphopenia and myeloproliferation due to elevated Interferon-gamma signals. Scientific reports. 2019; 9 12658 [PubMed: 31477755]
- 27. Hjelmeland AB, Wu Q, Wickman S, Eyler C, Heddleston J, Shi Q, Lathia JD, Macswords J, Lee J, McLendon RE, Rich JN, et al. Targeting A20 decreases glioma stem cell survival and tumor growth. PLoS biology. 2010; 8 e1000319 [PubMed: 20186265]
- 28. Dong B, Lv G, Wang Q, Wei F, Bellail AC, Hao C, Wang G. Targeting A20 enhances TRAIL-induced apoptosis in hepatocellular carcinoma cells. Biochemical and biophysical research communications. 2012; 418:433–438. [PubMed: 22285182]
- 29. Shao L, Oshima S, Duong B, Advincula R, Barrera J, Malynn BA, Ma A. A20 restricts wnt signaling in intestinal epithelial cells and suppresses colon carcinogenesis. PloS one. 2013; 8 e62223 [PubMed: 23671587]
- 30. Gyorffy B, Surowiak P, Budczies J, Lanczky A. Online survival analysis software to assess the prognostic value of biomarkers using transcriptomic data in non-small-cell lung cancer. PloS one. 2013; 8 e82241 [PubMed: 24367507]
- 31. Jackson EL, Willis N, Mercer K, Bronson RT, Crowley D, Montoya R, Jacks T, Tuveson DA. Analysis of lung tumor initiation and progression using conditional expression of oncogenic K-ras. Genes & development. 2001; 15:3243–3248. [PubMed: 11751630]
- 32. Hovelmeyer N, Reissig S, Xuan NT, Adams-Quack P, Lukas D, Nikolaev A, Schluter D, Waisman A. A20 deficiency in B cells enhances B-cell proliferation and results in the development of autoantibodies. European journal of immunology. 2011; 41:595–601. [PubMed: 21341261]
- 33. Wang X, Deckert M, Xuan NT, Nishanth G, Just S, Waisman A, Naumann M, Schluter D. Astrocytic A20 ameliorates experimental autoimmune encephalomyelitis by inhibiting NF-kappaB- and STAT1-dependent chemokine production in astrocytes. Acta neuropathologica. 2013
- 34. Liu J, Yang S, Wang Z, Chen X, Zhang Z. Ubiquitin ligase A20 regulates p53 protein in human colon epithelial cells. Journal of biomedical science. 2013; 20:74. [PubMed: 24099634]
- 35. Muzumdar MD, Dorans KJ, Chung KM, Robbins R, Tammela T, Gocheva V, Li CM, Jacks T. Clonal dynamics following p53 loss of heterozygosity in Kras-driven cancers. Nat Commun. 2016; 7 12685 [PubMed: 27585860]
- 36. Newman AM, Liu CL, Green MR, Gentles AJ, Feng W, Xu Y, Hoang CD, Diehn M, Alizadeh AA. Robust enumeration of cell subsets from tissue expression profiles. Nature methods. 2015; 12 :453–457. [PubMed: 25822800]
- 37. Girard L, Rodriguez-Canales J, Behrens C, Thompson DM, Botros IW, Tang H, Xie Y, Rekhtman N, Travis WD, Wistuba II, Minna JD, et al. An Expression Signature as an Aid to the Histologic Classification of Non-Small Cell Lung Cancer. Clinical cancer research an official journal of the American Association for Cancer Research. 2016; 22:4880–4889. [PubMed: 27354471]
- 38. Rooney MS, Shukla SA, Wu CJ, Getz G, Hacohen N. Molecular and genetic properties of tumors associated with local immune cytolytic activity. Cell. 2015; 160:48–61. [PubMed: 25594174]

39. Reiniger L, Teglasi V, Pipek O, Rojko L, Glasz T, Vagvolgyi A, Kovalszky I, Gyulai M, Lohinai Z, Raso E, Timar J, et al. Tumor necrosis correlates with PD-L1 and PD-1 expression in lung adenocarcinoma. Acta oncologica (Stockholm, Sweden). 2019; 58:1087–1094.

- 40. Blagih J, Zani F, Chakravarty P, Hennequart M, Pilley S, Hobor S, Hock AK, Walton JB, Morton JP, Gronroos E, Mason S, et al. Cancer-Specific Loss of p53 Leads to a Modulation of Myeloid and T Cell Responses. Cell Rep. 2020; 30:481–496. e486 [PubMed: 31940491]
- 41. Taniguchi T, Takaoka A. A weak signal for strong responses: interferon-alpha/beta revisited. Nature reviews Molecular cell biology. 2001; 2:378–386. [PubMed: 11331912]
- 42. Reilly SM, Chiang SH, Decker SJ, Chang L, Uhm M, Larsen MJ, Rubin JR, Mowers J, White NM, Hochberg I, Downes M, et al. An inhibitor of the protein kinases TBK1 and IKK-varepsilon improves obesity-related metabolic dysfunctions in mice. Nature medicine. 2013; 19:313–321.
- 43. Gough DJ, Messina NL, Hii L, Gould JA, Sabapathy K, Robertson AP, Trapani JA, Levy DE, Hertzog PJ, Clarke CJ, Johnstone RW, et al. Functional crosstalk between type I and II interferon through the regulated expression of STAT1. PLoS biology. 2010; 8 e1000361 [PubMed: 20436908]
- 44. Kamphuis E, Junt T, Waibler Z, Forster R, Kalinke U. Type I interferons directly regulate lymphocyte recirculation and cause transient blood lymphopenia. Blood. 2006; 108:3253–3261. [PubMed: 16868248]
- 45. Damotte D, Warren S, Arrondeau J, Boudou-Rouquette P, Mansuet-Lupo A, Biton J, Ouakrim H, Alifano M, Gervais C, Bellesoeur A, Kramkimel N, et al. The tumor inflammation signature (TIS) is associated with anti-PD-1 treatment benefit in the CERTIM pan-cancer cohort. J Transl Med. 2019; 17:357. [PubMed: 31684954]
- 46. Higgs BW, Morehouse CA, Streicher K, Brohawn PZ, Pilataxi F, Gupta A, Ranade K. Interferon Gamma Messenger RNA Signature in Tumor Biopsies Predicts Outcomes in Patients with Non-Small Cell Lung Carcinoma or Urothelial Cancer Treated with Durvalumab. Clinical cancer research an official journal of the American Association for Cancer Research. 2018; 24:3857– 3866. [PubMed: 29716923]
- 47. Grasso CS, Tsoi J, Onyshchenko M, Abril-Rodriguez G, Ross-Macdonald P, Wind-Rotolo M, Champhekar A, Medina E, Torrejon DY, Shin DS, Tran P, et al. Conserved Interferon-γ Signaling Drives Clinical Response to Immune Checkpoint Blockade Therapy in Melanoma. Cancer Cell. 2020; 38:500–515. e503 [PubMed: 32916126]
- 48. Shin DS, Zaretsky JM, Escuin-Ordinas H, Garcia-Diaz A, Hu-Lieskovan S, Kalbasi A, Grasso CS, Hugo W, Sandoval S, Torrejon DY, Palaskas N, et al. Primary Resistance to PD-1 Blockade Mediated by JAK1/2 Mutations. Cancer discovery. 2017; 7:188–201. [PubMed: 27903500]
- Ayers M, Lunceford J, Nebozhyn M, Murphy E, Loboda A, Kaufman DR, Albright A, Cheng JD, Kang SP, Shankaran V, Piha-Paul SA, et al. IFN-gamma-related mRNA profile predicts clinical response to PD-1 blockade. The Journal of clinical investigation. 2017; 127:2930–2940. [PubMed: 28650338]
- 50. Sucker A, Zhao F, Pieper N, Heeke C, Maltaner R, Stadtler N, Real B, Bielefeld N, Howe S, Weide B, Gutzmer R, et al. Acquired IFNγ resistance impairs anti-tumor immunity and gives rise to T-cell-resistant melanoma lesions. Nat Commun. 2017; 8 15440 [PubMed: 28561041]
- 51. Gide TN, Quek C, Menzies AM, Tasker AT, Shang P, Holst J, Madore J, Lim SY, Velickovic R, Wongchenko M, Yan Y. Distinct Immune Cell Populations Define Response to Anti-PD-1 Monotherapy and Anti-PD-1/Anti-CTLA-4 Combined Therapy. Cancer Cell. 2019; 35:238–255. e236 [PubMed: 30753825]
- 52. Greten FR, Grivennikov SI. Inflammation and Cancer: Triggers, Mechanisms, and Consequences. Immunity. 2019; 51:27–41. [PubMed: 31315034]
- 53. Meylan E, Dooley AL, Feldser DM, Shen L, Turk E, Ouyang C, Jacks T. Requirement for NF-kappaB signalling in a mouse model of lung adenocarcinoma. Nature. 2009; 462:104–107. [PubMed: 19847165]
- 54. Basseres DS, Ebbs A, Cogswell PC, Baldwin AS. IKK is a therapeutic target in KRAS-Induced lung cancer with disrupted p53 activity. Genes Cancer. 2014; 5:41–55. [PubMed: 24955217]

 Basseres DS, Ebbs A, Levantini E, Baldwin AS. Requirement of the NF-kappaB subunit p65/ RelA for K-Ras-induced lung tumorigenesis. Cancer research. 2010; 70:3537–3546. [PubMed: 20406971]

- 56. Xue W, Meylan E, Oliver TG, Feldser DM, Winslow MM, Bronson R, Jacks T. Response and resistance to NF-kappaB inhibitors in mouse models of lung adenocarcinoma. Cancer discovery. 2011; 1:236–247. [PubMed: 21874163]
- 57. Liu Y, Zhang X, Han C, Wan G, Huang X, Ivan C, Jiang D, Rodriguez-Aguayo C, Lopez-Berestein G, Rao PH, Maru DM, et al. TP53 loss creates therapeutic vulnerability in colorectal cancer. Nature. 2015; 520:697–701. [PubMed: 25901683]
- 58. Gough DJ, Messina NL, Clarke CJ, Johnstone RW, Levy DE. Constitutive type I interferon modulates homeostatic balance through tonic signaling. Immunity. 2012; 36:166–174. [PubMed: 22365663]
- 59. Boone DL, Turer EE, Lee EG, Ahmad RC, Wheeler MT, Tsui C, Hurley P, Chien M, Chai S, Hitotsumatsu O, McNally E, et al. The ubiquitin-modifying enzyme A20 is required for termination of Toll-like receptor responses. Nature immunology. 2004; 5:1052–1060. [PubMed: 15334086]
- 60. Lin CF, Lin CM, Lee KY, Wu SY, Feng PH, Chen KY, Chuang HC, Chen CL, Wang YC, Tseng PC, Tsai TT. Escape from IFN-gamma-dependent immunosurveillance in tumorigenesis. Journal of biomedical science. 2017; 24:10. [PubMed: 28143527]
- 61. Meissl K, Macho-Maschler S, Muller M, Strobl B. The good and the bad faces of STAT1 in solid tumours. Cytokine. 2017; 89:12–20. [PubMed: 26631912]
- 62. McFadden DG, Politi K, Bhutkar A, Chen FK, Song X, Pirun M, Santiago PM, Kim-Kiselak C, Platt JT, Lee E, Hodges E, et al. Mutational landscape of EGFR-, MYC-, and Kras-driven genetically engineered mouse models of lung adenocarcinoma. Proceedings of the National Academy of Sciences of the United States of America. 2016; 113:E6409–e6417. [PubMed: 27702896]
- 63. DuPage M, Cheung AF, Mazumdar C, Winslow MM, Bronson R, Schmidt LM, Crowley D, Chen J, Jacks T. Endogenous T cell responses to antigens expressed in lung adenocarcinomas delay malignant tumor progression. Cancer Cell. 2011; 19:72–85. [PubMed: 21251614]
- 64. de Carné Trécesson S, Boumelha J, Law EK, Romero-Clavijo P, Mugarza E, Coelho MA, Moore C, Rana S, Caswell DR, Murillo M, Hancock DC, et al. APOBEC3B expression generates an immunogenic model of Kras mutant lung cancer. bioRxiv. 2020 2020.2012.2022.423126
- 65. Cubas R, Moskalenko M, Cheung J, Yang M, McNamara E, Xiong H, Hoves S, Ries CH, Kim J, Gould S. Chemotherapy Combines Effectively with Anti-PD-L1 Treatment and Can Augment Antitumor Responses. Journal of immunology (Baltimore, Md.: 1950). 2018; 201:2273–2286.
- 66. Pfirschke C, Engblom C, Rickelt S, Cortez-Retamozo V, Garris C, Pucci F, Yamazaki T, Poirier-Colame V, Newton A, Redouane Y, Lin YJ, et al. Immunogenic Chemotherapy Sensitizes Tumors to Checkpoint Blockade Therapy. Immunity. 2016; 44:343–354. [PubMed: 26872698]
- 67. Srivastava S, Furlan SN, Jaeger-Ruckstuhl CA, Sarvothama M, Berger C, Smythe KS, Garrison SM, Specht JM, Lee SM, Amezquita RA, Voillet V, et al. Immunogenic Chemotherapy Enhances Recruitment of CAR-T Cells to Lung Tumors and Improves Antitumor Efficacy when Combined with Checkpoint Blockade. Cancer Cell. 2021; 39:193–208. e110 [PubMed: 33357452]

One Sentence Summary

A20 represents an immune checkpoint in lung adenocarcinomas, and its loss is compensated by targeting the TBK1-STAT1-PD-L1 axis.

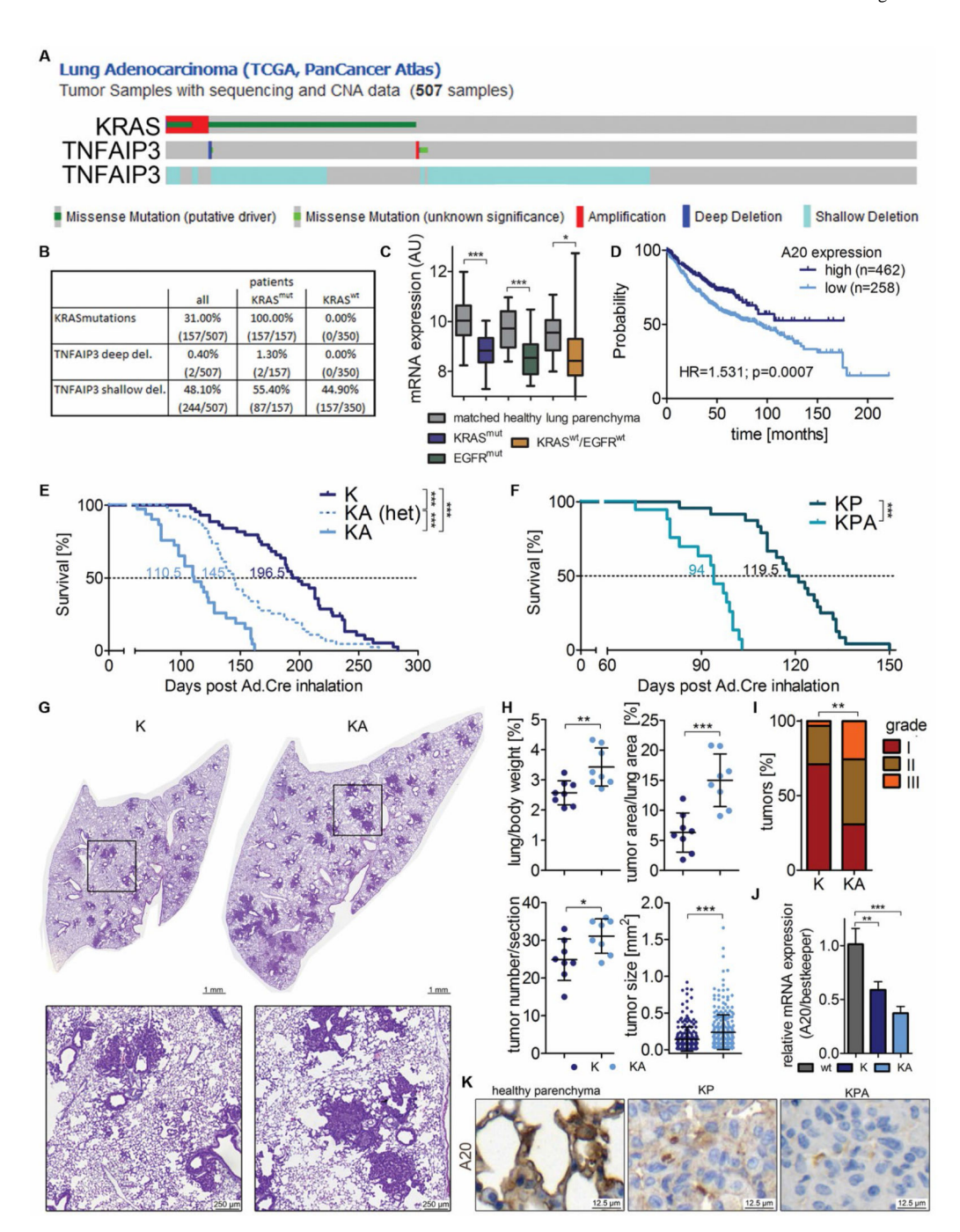


Figure 1. A20 is a tumor suppressor in K-RAS driven lung tumorigenesis.

(A) Oncoprint of LUAD depicting patients harboring K-RAS mutations, as well as mutations and deletions of TNFAIP3 and (B) quantitation of patients harboring alterations in these genes. Data were derived from the TCGA PanCancer Atlas. (C) Relative A20 mRNA expression in K-RAS mutant, EGFR mutant and K-RAS wildtype/EGFR wildtype LUAD biopsies compared to adjacent healthy lung tissue of the same individuals. Data was retrieved from the Gene Expression Omnibus (GSE75037) and analyzed using student's t test, Box plot with min to max whiskers, n=35 for K-RAS^{mut}, 20 for

EGFR^{mut} and 21 for K-RAS^{wt}/EGFR^{wt}. AU, arbitrary units. (**D**) Kaplan Meier plot showing overall survival of patients with LUAD stratified by high (n=258) and low (n=462) A20 expression. Univariate cox regression test was used for statistical analysis. (E) Survival analysis of K-ras^{G12D} (K, n=42), K-ras^{G12D}:A20 Lep/ Lep (KA, n=28) and K-ras^{G12D}:A20 Lep/+ [KA (het) n=48] mice and (**F**) of K-ras^{G12D}:p53 Lep/ Lep (KP, n=24) versus K-ras^{G12D}:p53 Lep/ Lep/ Lep/ Lep (KPA, n=16) mice following intranasal inhalation with Ad.CMV-Cre. Statistical analysis was performed using the Log rank test. (G) Representative pictures of H&E stained sections from tumor bearing lungs 10 weeks following Ad.CMV-Cre inhalation of K and KA mice, including higher magnification of indicated areas, Scale bars, 1 mm (top) and 250 µm (bottom). (H) Graphs depict lung to body weight rations, tumor area versus healthy lung area and tumor number per analyzed section in K and KA mice (n=8 per group), as well as the area of all tumors found in analyzed sections (n=227 for K and n=292 for KA mice). Data was analyzed using student's t test. (I) Graph indicates the percentage of stage I, stage II and stage III tumors, respectively, in K versus KA mice (n=4 sections per group). (J) A20 mRNA expression in tumor free wildtype lungs (wt) compared to tumor bearing lungs of K and KA mice, 10 weeks post Ad.CMV-Cre inhalation. Data was analyzed by Oneway ANOVA, n=4 per group. (K) Representative images of stainings for A20 in the healthy parenchyma and in the tumors of lungs of KP mice and KPA mice. *p<0.05, **p<0.01, ***p<0.001. Graphs in (H) & (J) depict means \pm SD.

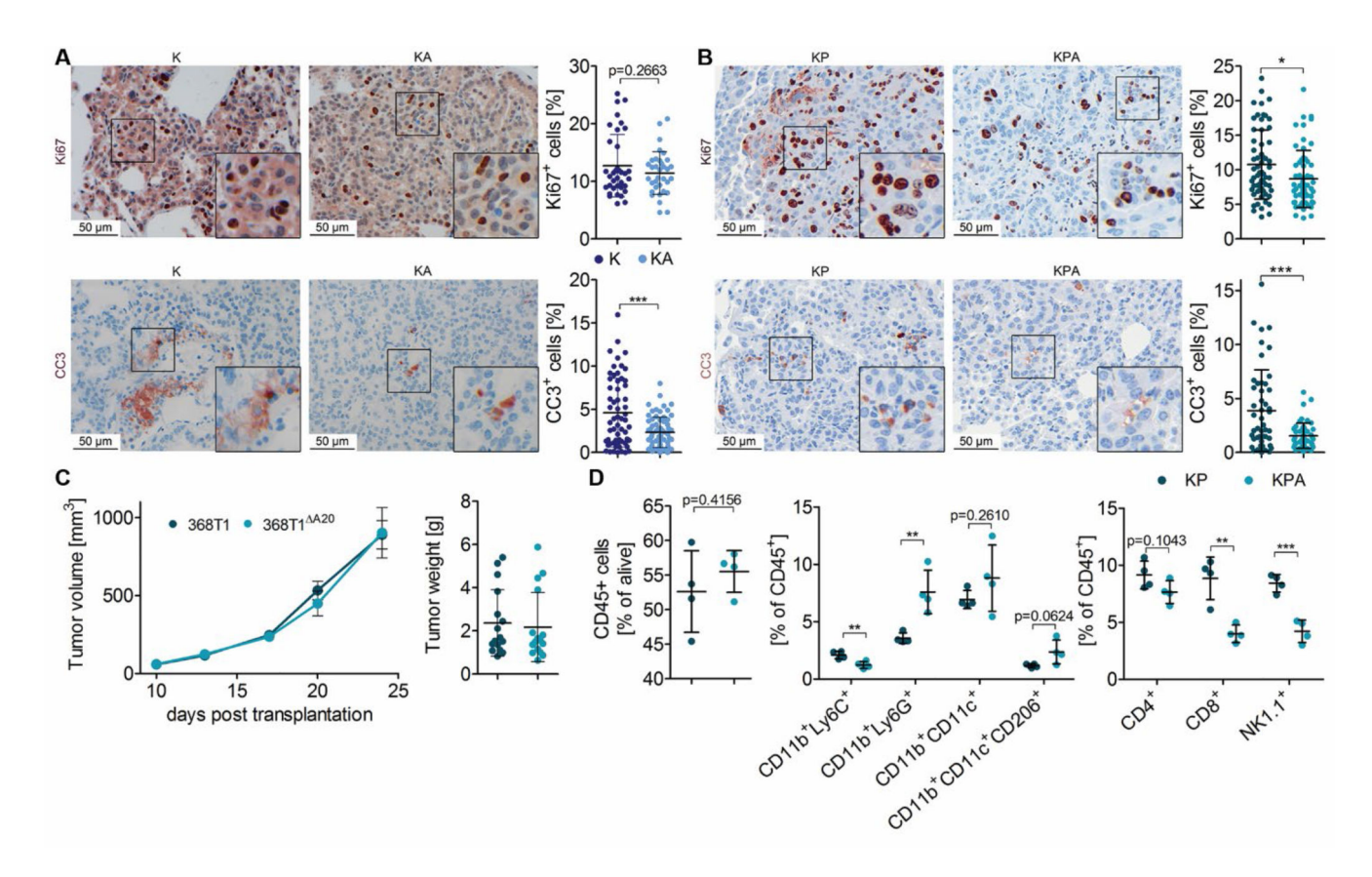


Figure 2. Loss of A20 alters tumor immune cell infiltration.

(A) Representative images of immunohistochemical stainings for Ki67 and cleaved Caspase 3 (CC3) in lung tumors of K-ras G12D (K) and K-ras G12D :A20 Lep/ Lep (KA) mice and of (B) K-ras G12D :p53 Lep/ Lep (KP) and K-ras G12D :p53 Lep/ Lep (KPA) mice. Percentage of positively stained cells in at least eight individual tumors per mouse was evaluated using TissueGnostics software, n= 5 to 7 mice per group, scale bars, 50 μ m.(C) Volumes as measured with a caliper of engrafted tumor-derived from A20-expressing versus A20-deficient 368T1 cells in NSG mice, monitored over 4 weeks. The graph at the right depicts the weight of the individual tumors after 4 weeks (n=16 per group). (D) Flow cytometric analysis of cell suspensions derived from tumor bearing lungs of KP versus KPA mice (n= 4 per group). Statistical analysis was performed using the student's t test. Graphs represent means \pm SD. *p<0.05, **p<0.01, ***p<0.001.

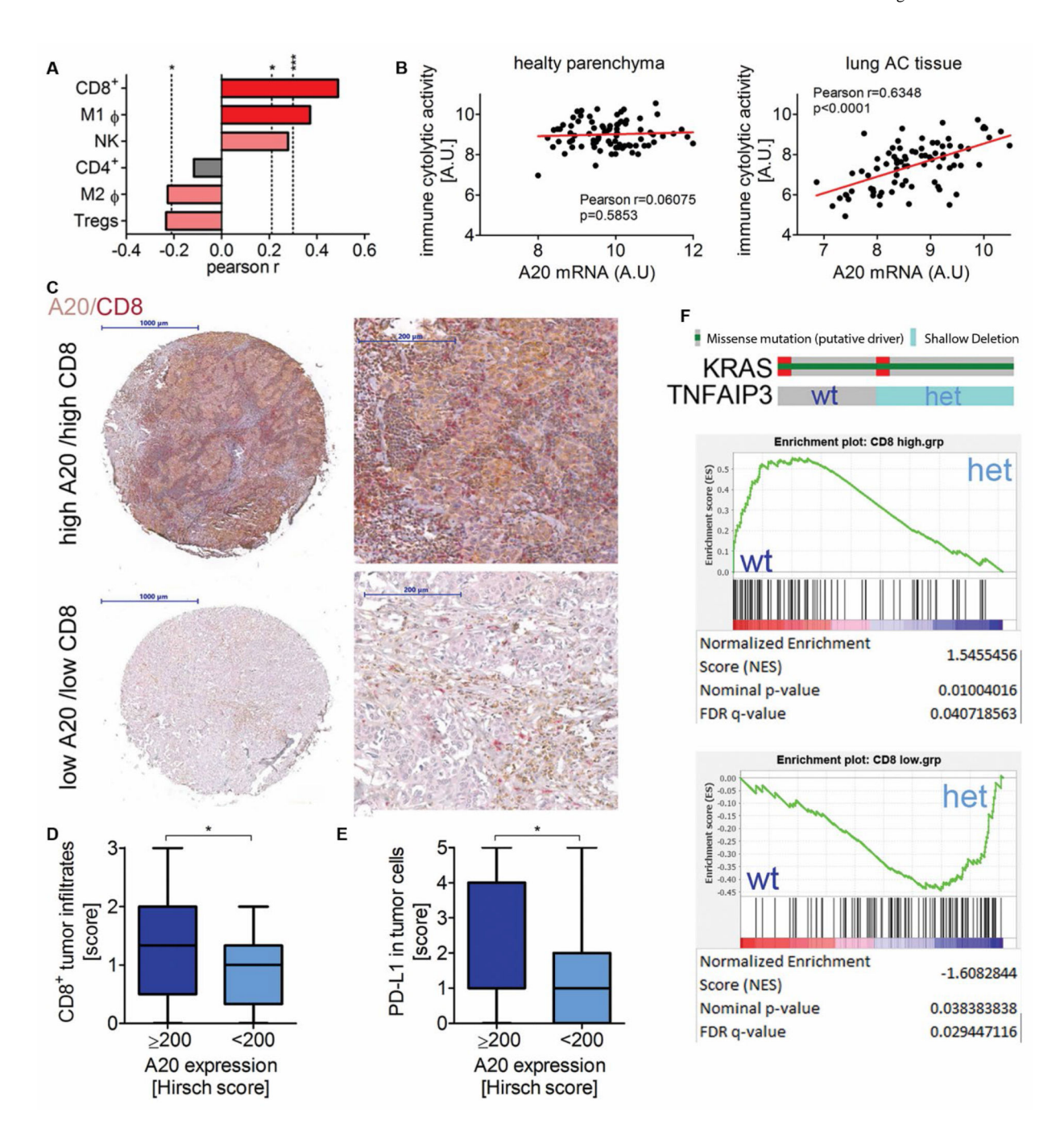


Figure 3. A20 expression positively correlates with cytotoxic T cell infiltration in LUAD patients. (**A**) The abundance of indicated immune cell-types in LUAD biopsies was evaluated by CIBERSORT and correlated with respective A20 mRNA expression values. Data was derived from GSE75037. The graph depicts the Pearson correlation coefficient for different cell-types, dotted lines indicate significance levels < 0.05 (*) and < 0.001 (***), respectively. (**B**) Graphs depict mRNA expression values for A20 versus immune cytolytic activity as calculated by the mean of *GZMA* and *PRF1* expression, in healthy lung parenchyma (left panel) and in LUAD biopsies of the same cohort (right panel). Data were derived from

GSE75037. (**C**) Images from LUAD biopsies spotted on a tissue micro array and following immunohistochemical staining for A20 (brown color) and CD8 (red color). The displayed pictures are representative for samples with high versus low A20 expression. Scale bars: 1 mm (left panel) and 200 µm (right panel). n=84. (**D**) Graph depicts scoring for CD8⁺ T cell infiltrates in LUAD biopsies exhibiting an A20 Hirsch score (percentage of positive tumor cells x staining intensity) equal and above to 200 (n=57) versus below 200 (n=27). Box plot with min to max whiskers, and data was analyzed using the student's t test.

*p<0.05 (**E**) Scoring of PD-L1 expression of tumor cells in LUAD biopsies stratified by A20 Hirsch score. *p<0.05 (**F**) Gene set enrichment analysis of expression data derived from TCGA PanCancer Atlas and for LUAD patients harboring K-RAS mutations, discriminating between patients with no alterations in the TNFAIP3/A20 gene (WT; n=61) versus patients with shallow deletions of TNFAIP3 (HET, n=79). Gene sets were generated using the top 100 genes positively (CD8_high_100) or negatively (CD8_low_100) correlating with CD8 abundance in LUAD samples as evaluated by CIBERSORT analysis of GSE75037 dataset.

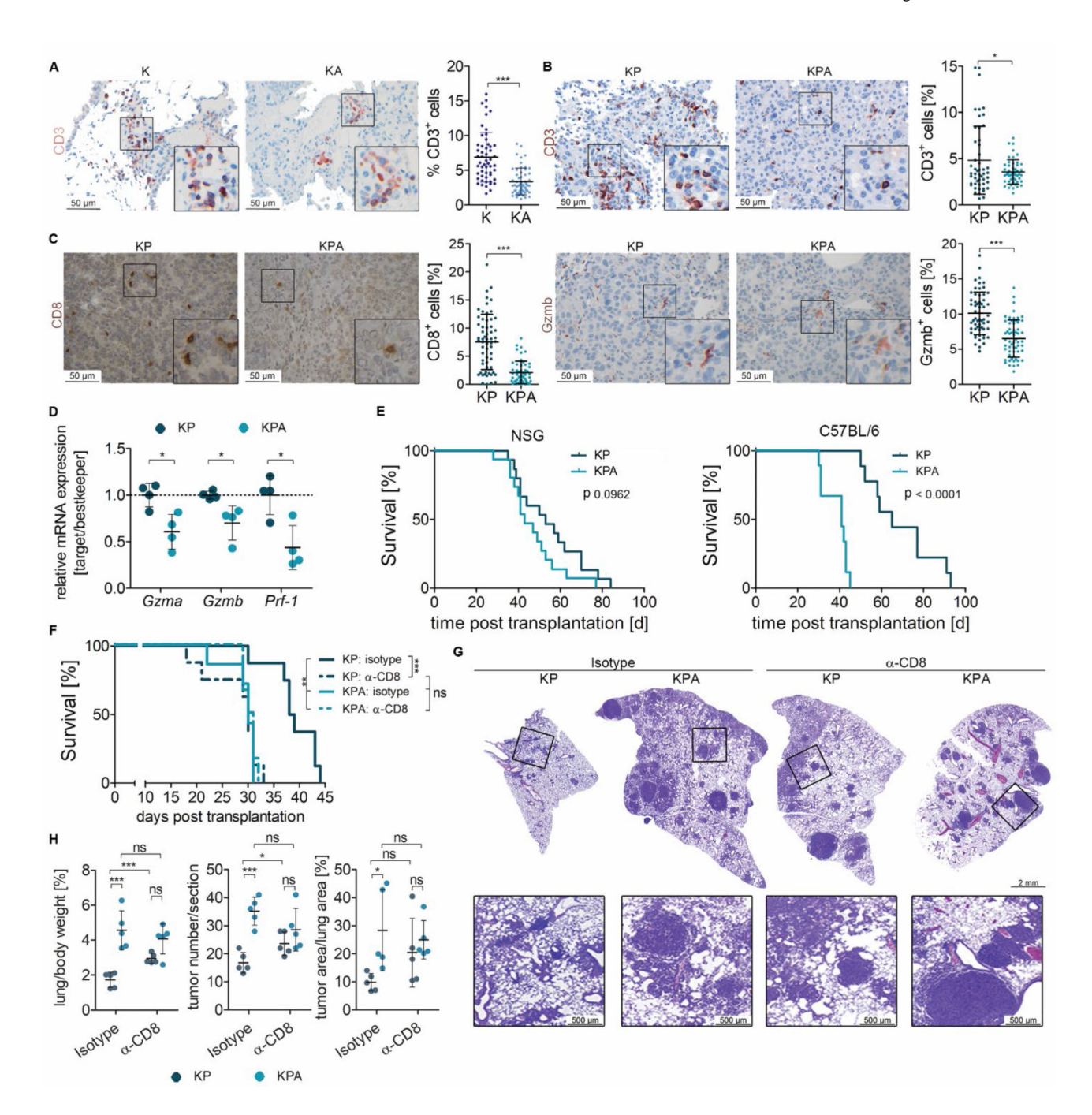


Figure 4. Increased tumorigenicity of A20 knockout LUAD depends on evasion of CD8+ T cells. (**A**) Representative images and quantitation of immunohistochemical stainings for CD3 in tumors of K-ras^{G12D} (K) versus K-ras^{G12D}:A20 Lep/ Lep (KA) and (**B**) K-ras^{G12D}:p53 Lep/ Lep (KP) versus K-ras^{G12D}:p53 Lep/ Lep:A20 Lep/ Lep (KPA) mice (right panels). Data was analyzed using student's t test and bars indicate means ± SD. *p<0.05, ***p<0.001. (**C**) Representative images of CD8 and granzyme B stainings (Gzmb) in lung tumors of KP and KPA mice, 10 weeks post tumor initiation. Graph depicts percentage of positive cells within the tumor for respective stainings, and more than 10 tumors were

analyzed per lung (n=4 mice per group). Scale bars, 50 µm. (**D**) Quantitation of normalized mRNA expression levels for indicated genes from lysates of tumor bearing lungs of K-ras $^{\rm G12D}$:p53 $^{\rm Lep/}$ Lep (KP) and K-ras $^{\rm G12D}$:p53 $^{\rm Lep/}$ Lep (KPA) mice. n=4 per group. (**E**) Survival analysis of NSG mice (left panel, n=15 per group) and C57Bl/6 mice (right panel, n=9 per group) following orthotopic transplantation of KP and KPA tumor cells. Log rank test was used for statistical analysis. (**F**) Survival analysis of C57Bl/6 mice after orthotopic transplantation with KP and KPA cells, and antibody mediated CD8+ T cell depletion started one week post tumor cell engraftment. Isotype antibody was used as control. Data was analyzed by Log rank test. (n=6-8 mice per group). (**G**) Images of lungs from KP and KPA mice 10 weeks post Ad.SPC-Cre inhalation and following treatment with CD8 depleting antibodies versus isotype controls. Lower panel shows higher magnification of indicated sections, scale bar, 2 mm and 500 µm. (**H**) Graphs depict lung to body weight ratios, tumor numbers per analyzed sections and the percentage of tumor area to total lung area. n=5 per group. (**A**), (**B**), (**C**) & (**H**) Bars indicate means \pm SD, and data was analyzed using student's t test. *p<0.05, ***p<0.001.

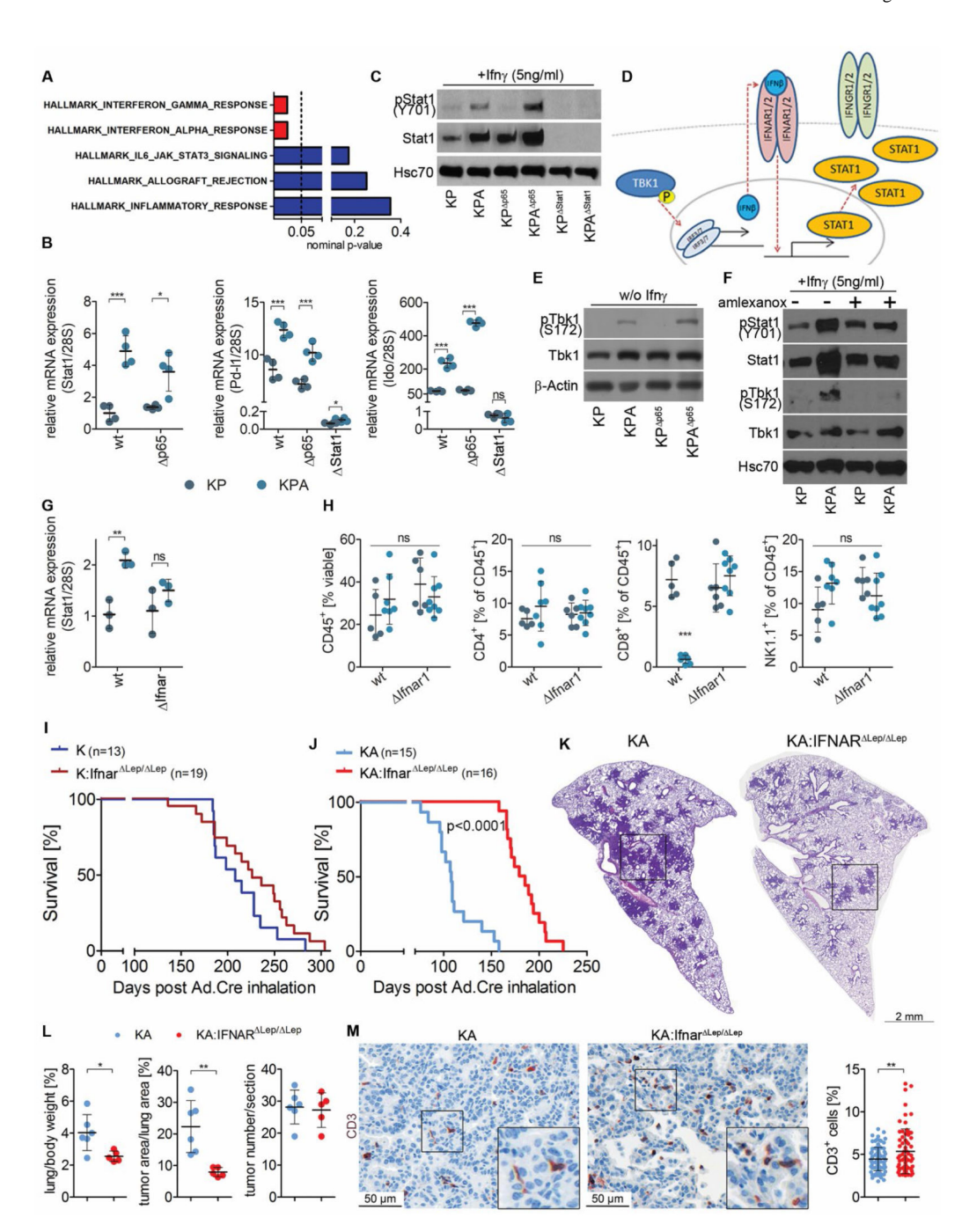


Figure 5. Autocrine IFN signaling enables aberrant growth of A20 knockout LUAD. (A) Graph depicts the nominal p-value of all hallmark gene sets enriched in KPA tumors with a normalized enrichment score > 1 as compared to KP tumors. RNAseq data of macroscopically dissected lung tumors in K-ras G12D :p53 $^{Lep/Lep}$ (KP) versus K-ras G12D :p53 $^{Lep/Lep}$:A20 $^{Lep/Lep}$ (KPA) mice 10 weeks post Ad.Cre administration was used for the hallmark gene set enrichment analysis. (B) Stat1 mRNA expression in untreated wildtype (wt) and p65 deficient K-ras G12D :p53 $^/$ (KP) and K-ras G12D :p53 $^/$:A20 $^/$ (KPA) cells, and Pd-l1 and Ido mRNA fold increase upon 4 hours treatment with Ifnγ

in KP and KPA cells, with and without p65 and Stat1 knockout. 28S expression was used for normalization, and fold levels were calculated to expression in untreated KP cells. (C) Western blots for indicated (phospho-) proteins using cell lysates of p65 expressing and deficient KP and KPA cells, respectively. Cells were stimulated with Ifny for 10 minutes. (**D**) Scheme illustrating the feed forward loop involving TBK1 activation, IFNβ expression and autocrine signaling via the IFNa receptor resulting in STAT1 expression for IFNγ mediated responses. (E) Western blot probing for indicated proteins in cell lysates of untreated KP and KPA cells, with and without p65 knockout, and (F) in amlexanox treated (48 hours) KP and KPA cells following 10 minutes Ifny treatment. (G) Relative Stat1 mRNA expression in wt and Ifnar1 deficient KP and KPA cells. (H) Quantitation by flow cytometry of indicated immune cells in lungs of C57Bl/6 mice, two weeks following orthotopic transplantation of KP and KPA cells, with and without Ifnar1 deletion (n=5-8 mice per group). (I) Kaplan Maier analysis of Ad.SPC-Cre inhaled K mice versus K mice with additional Ifnar deletion in tumor cells (K:Ifnar Lep/ Lep) and (J) KA mice versus KA:Ifnar Lep/ Lep, n=13-19 mice per group. Log rank test was performed for statistical analysis. (K) H&E stained sections of lungs in KA and KA:Ifnar Lep/ Lep mice, 10 weeks post Ad.SPC-Cre inhalation. Lower panel shows a higher magnification of indicated lung areas. (L) Graph depicts means \pm SD of lung to body weight and tumor area to total lung area ratios, and tumor numbers per analyzed section, n 5. (M) Representative CD3 immunohistochemical stainings and quantitation (means \pm SD) for T cell infiltration in tumors of KA and KA:Ifnar Lep/ Lep mice, 10 weeks after tumor initiation with Ad.SPC-Cre inhalation. (B), (G) & (L) were analyzed using student's t test, (H) by One way ANOVA, bars indicate means \pm SD.*p<0.05, **p<0.01, ***p<0.001.

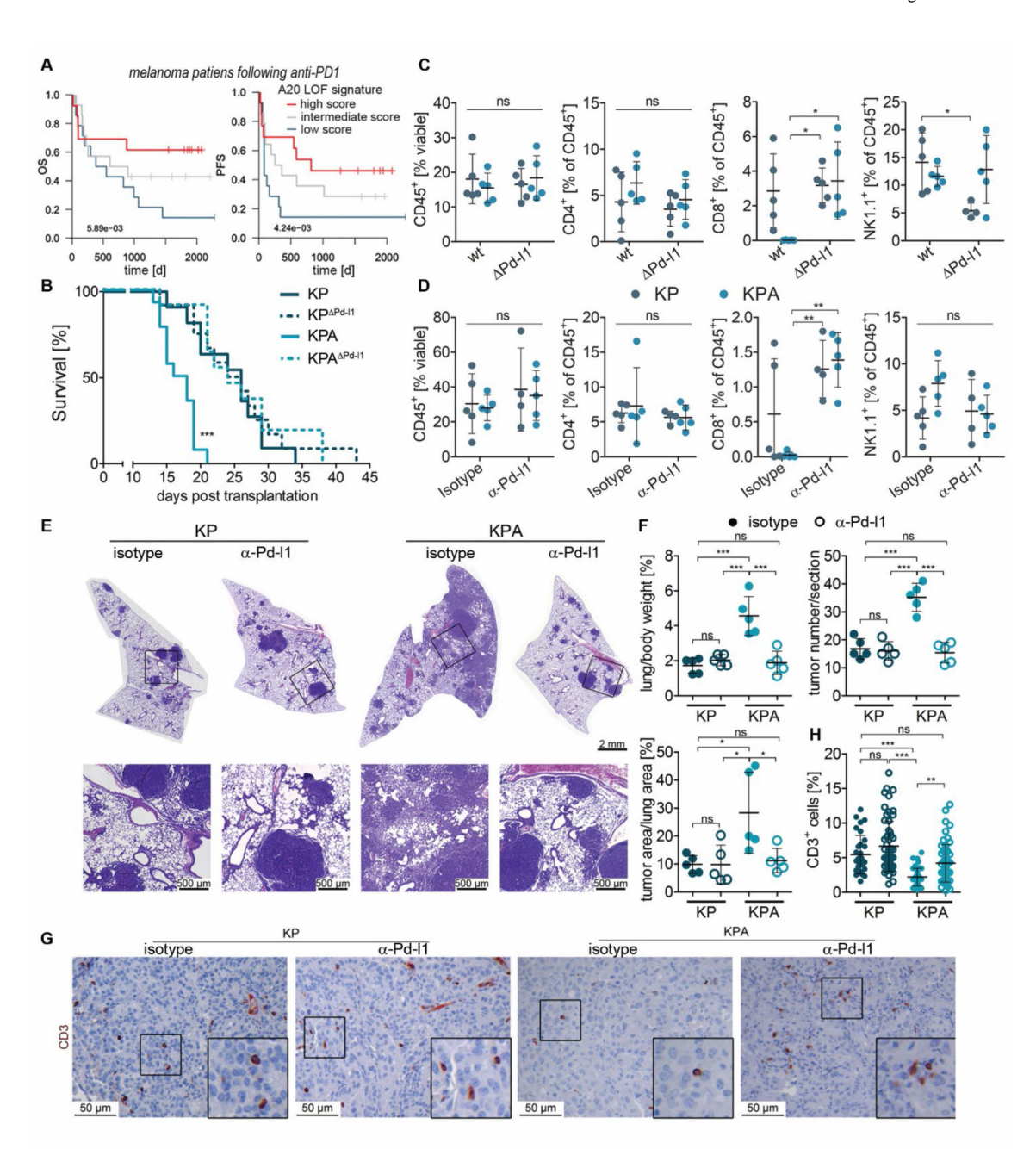


Figure 6. A20 deficiency sensitizes LUAD to anti-PD-L1 therapy.

(A) Overall survival (OS) and progression free survival (PFS) of melanoma patients treated with anti-PD-1 monotherapy stratified according to the A20 LOF signature score (high n=13, intermediate n=14, low n=14). Data was analyzed by Log rank test. (B) Kaplan Meier analysis of C57Bl/6 mice following orthotopic transplantation with indicated cell lines. Log rank test was performed for statistical analysis. (C) Quantitation of indicated immune cells in lungs of syngeneic recipients from orthotopic transplants of KP and KPA cells, with and without Pd-11 knock-out, (D) or treated with anti-Pd-11 antibody or isotype controls. Lungs

were harvested two weeks post transplantation. (n=4-5 mice per group). Data was analyzed by One-way ANOVA. (**E**) H&E stained lung sections of KP and KPA mice treated with indicated antibodies over the experimental period of 10 weeks and (**F**) quantification of lung to body weight ratios, tumor numbers per section and tumor area to total lung area of these mice. Data was analyzed using One-way ANOVA. Experiment was performed together with the antibody mediated CD8 depletion in Fig. 4G–H, hence isotype control group is the same. (**G**) Representative CD3 immunohistochemical stainings and (**H**) quantification for infiltrating CD3 positive T cells in tumors of KP and KPA mice, 10 weeks after tumor initiation and treatment with anti-PD-L1 antibody or isotype controls. (**B**), (**C**), (**D**), (**F**) & (**H**) Graphs show means \pm SD. *p<0.05, **p<0.01, ***p<0.001.